Available online at www.sciencedirect.com
SCIENCE DIRECT
Polymer 46 (2005) 8386–8395
polymer
www.elsevier.com/locate/polymer

Flame retardant mechanism of polymer/clay nanocomposites based on polypropylene

Huaili Qin, Shimin Zhang, Chungui Zhao, Guangjun Hu, Mingshu Yang*

CAS Key Laboratory of Engineering Plastics, Joint Laboratory of Polymer Science and Materials, Institute of Chemistry, Chinese Academy of Sciences, Beijing 100080, People's Republic of China

Received 7 April 2005; received in revised form 15 June 2005; accepted 5 July 2005

Abstract

The combustion behavior and thermal-oxidative degradation of polypropylene/clay nanocomposite has been studied in this paper. The influence of compatibilizer, alkylammonium, organoclay, protonic clay and pristine clay is considered, respectively. The decrease of heat release rate (HRR) is mainly due to the delay of thermal-oxidative decomposition of the composites. The active sites on clay layers can catalyze the initial decomposition and the ignition of the composites. On the other hand, the active sites can catalyze the formation of a protective coating char on the samples. Moreover, the active sites can catalyze the dehydrogenation and crosslinking of polymer chains. Accordingly, the thermal-oxidative stability is increased and HRR is decreased.

Keywords: Polypropylene; Nanocomposite; Flame retardant

1. Introduction

The research and development of flame retardant polymeric materials always receives great attention whether in fundamental research or industry exploitation. Recent advances in flame retardant polymeric materials have centered on the flame retardancy of polymer/clay nanocomposites (PCN). Adding just a tiny amount of clay to the polymer matrix, these new-generation of composite materials exhibit significant decrease in the peak heat release rate (PHRR), change in the char structure, and decrease in the mass loss rate during combustion in the cone calorimeter [1–13]. It does not have the usual drawbacks associated with other fire retardant additives. Moreover, PCN materials increase physical, thermal and mechanical properties dramatically [14–21]. It pushes ahead with the development of flame retardant polymeric materials, which is commended as a revolutionary new flame retardant approach.

Several mechanisms have been proposed to describe the flame retardant properties of PCN. The general view of the flame retardant mechanism is that a carbonaceous silicate char builds up on the surface during burning which creates a protective barrier to heat and mass transfer [3,6,8]. The accumulation of layered silicates on the burning/gasifying sample surface is considered due to two possible modes [8]. One is that the layered silicates left on the sample surface as the result of the decomposition of the polymer matrix by pyrolysis. The other is that the transportation of the layered silicates pushed by numerous rising bubbles of degradation products and the associated convection flow in the melt from the interior of the sample toward the surface. Wilkie et al. [5] have also proposed a mechanism that paramagnetic irons within clay could function as radical traps to prevent degradation. Their results showed that even when the fraction of clay was as low as 0.1%, the PHRR is lower by 40%, a value not much different from that observed at high amounts of clay. It seems that the barrier effect is not the only factor at such low loading of clay to lead to the great reduction of PHRR.

In our previous work [9,10], the thermal stability and flammability of polyamide 66/montmorillonite nanocomposites and polypropylene/montmorillonite (PP/MMT) composites have been reported. Even though the clay is not nano-dispersed in the cases of microcomposites, the

* Corresponding author. Tel.: +86 1 82615665.
E-mail address: yms@iccas.ac.cn (M. Yang).

0032-3861/$ - see front matter © 2005 Elsevier Ltd. All rights reserved.
doi:10.1016/j.polymer.2005.07.019

composites exhibit higher thermal stability and lower PHRR. It is likely due to not only the barrier effect, but also the physical–chemical effect of clay layers. Furthermore, we found that the addition of clay can catalyze the initial decomposition of PP matrix and accelerate the ignition of PP matrix in combustion.

Although great progress has been made, some issues are still unresolved on the mechanisms of flame retardancy observed for polymer/clay composite materials. What is the essential effect of the layered silicates on the reduction of PHRR for PCN? How does the dispersion state of clay influence the flammability of PCN? How is the inherent relation between thermal-oxidative degradation and combustion for PCN?

In the present work, PP/clay nanocomposite and several microcomposites were prepared to investigate their combustion behaviors by cone calorimeter. The influence of compatibilizer, alkylammonium, organoclay, protonic clay and pristine clay is considered, respectively. The char layer formed during combustion and the char residue were characterized. Moreover, the role of thermal-oxidative decomposition during combustion was also discussed by thermal gravimetric analysis (TGA).

2. Experimental

2.1. Materials

The isotactic polypropylene, 1300, was purchased from Yanshan Petrochemical Co. Ltd, Beijing, China. The maleic anhydride-grafted-polypropylene copolymer (melt index 30 g/10 min, amount of MA 0.8%, termed PP-*g*-MA) was purchased from Shanghai Genius Advanced Material Co. Ltd, Shanghai, China. Octadecyltrimethyl ammonium chloride [$C_{18}H_{37}N^+(CH_3)_3Cl^-$, denoted with C18] was purchased from Beijing Chemical Reagent Co., Beijing, China. Sodium montmorillonite (Na-MMT), with cation exchange capacity (CEC) of 90 mequiv/100 g, was purchased from Zhangjiakou Qinghe Chemical Factory, Hebei, China. Organic clay (termed OMMT) and protonic clay (termed H-MMT) were prepared as previously described [22]. OMMT was obtained by cation-exchanged with dioctadecyldimethyl ammonium chloride [$(C_{18}H_{37})_2N^+(CH_3)_2Cl^-$, denoted with 2C18], while H-MMT contained acidic sites H^+ within clay galleries.

2.2. Preparation of PP compounds

PP compounds were prepared using a twin-screw extruder as reported previously [22]. Their compositions are listed in Table 1. In the PP/C18 blend, the C18 content is 1.2 wt%, equivalent to the molar fraction of 2C18 in the PP/OMMT microcomposite. The dried pellets of the compounds were injection molded into $70\times70\times7$ mm^3 specimens. Samples of pure polymer were processed in the same way and used for comparison.

2.3. Thermal and combustion tests

The thermal-oxidative degradation was determined by thermal gravimetric analysis (TGA) using a Perkin–Elmer 7 series apparatus with a heating rate of 20 °C/min in air. The isothermal degradation experiment was performed at 200 °C in static air.

Combustion experiments were performed in a cone calorimeter (Fire Testing Technology, UK) at an incident heat flux of 35 kW/m^2. Peak heat release rate (PHRR), effective heat combustion (EHC), total heat evolved, specific extinction area (SEA), CO and CO_2 yield data were reproducible when measured at 35 kW/m^2 flux.

2.4. Characterization of char layer and char residue

Scanning electron microscopy (SEM), Fourier-transformed infrared spectroscopy (FT-IR) and X-ray diffraction (XRD) were used to characterize the char layer formed prior to ignition and char residue of the nanocomposite. SEM photographs of the char layer and the char residue of the nanocomposite were taken on a Hitachi S-430 field emission scanning electron microscopy using an accelerating voltage of 15 kV. The SEM samples were coated with gold. FT-IR spectra were recorded with KBr pellets on a Perkin–Elmer System 2000 Fourier-transformed infrared spectrometer. XRD patterns were obtained using a Rigaku (Japan) D/max 2400 diffractometer with Cu Kα radiation ($\lambda=0.154$ nm, 40 kV, 120 mA) at room temperature. The diffractograms

Table 1
The PP compounds and their composition

Sample	PP (wt%)	PP-*g*-MA (wt%)	Clay type and content		C18 (wt%)
			Type	(wt%)	
PP	100				
PP/Na-MMT	95		Na-MMT	5	
PP/OMMT	95		OMMT	5	
PP/H-MMT	95		H-MMT	5	
PP/C18	98.8				1.2
PP/PP-*g*-MA	85	15			
PP/PP-*g*-MA/OMMT	80	15	OMMT	5	

were scanned from 1.5 to 40° (2θ) in steps of 0.02° using a scanning rate of 8 °/min.

3. Results

3.1. Sample morphology

The TEM images of different types of PP/clay composites are shown in Fig. 1. Large and unevenly dispersed primary clay particles were observed in PP/Na-MMT composite (Fig. 1(A)), strongly suggesting an immiscible dispersion. The dispersion state of clay particles in PP/H-MMT (Fig. 1(B)) is similar to that in PP/Na-MMT, while clay particle in PP/OMMT (Fig. 1(C)) is much smaller than that in PP/Na-MMT. With the addition of PP-*g*-MA, partially exfoliated clay layers are present in PP/PP-*g*-MA/OMMT nanocomposite (Fig. 1(D)).

3.2. Combustion and thermal-oxidative degradation

The burning behavior of polymeric materials is understood in terms of their ability to generate flammable volatile products under the action of heat and their subsequent ignition. Accordingly, the combustion of organic polymers is a complicated process consisting of two stages: Thermal-oxidative degradation and normal burning [23,24]. The burning process involves a series of steps, such as heat transfer, thermal-oxidative decomposition to generate flammable volatile products, diffusion of gaseous products in solid state and gas state, combustion reaction of mixture involving volatiles and oxygen.

The combustion properties of the samples were characterized by means of cone calorimetry. Some of the cone calorimetric data for the PP compounds are shown in Table 2. It can be seen that the effective heat combustion (EHC), total heat evolved, average CO and CO_2 yield of the compounds show similar value to those of pure PP. Specific extinction area (SEA, a measure of smoke yield) of the compounds have a ca. 15% increase compared to that of pure PP. However, the peak heat release rate (PHRR) of the nanocomposite and other compounds is reduced in different degree (The HRR plots is shown in Figs. 2 and 6). This suggests that the improved flammability properties of these materials are due to difference in condensed-phase decomposition processes and not to a gas-phase effect [3,5,6]. That is to say, the flame retardant mechanism of PP/clay nanocomposite is associated with two decisive factors: One is thermal-oxidative degradation of the matrix, the other is diffusion of volatile decomposed products and heat transfer in the condensed-phase.

3.2.1. The influence of organoclay and compatibilizer

The HRR plots for pure PP, PP/PP-*g*-MA blend, PP/OMMT microcomposite and PP/PP-*g*-MA/OMMT nanocomposite are shown in Fig. 2. PP/PP-*g*-MA blend behaves very similarly to pure PP. The PHRR of PP/PP-*g*-MA/OMMT nanocomposite is dramatically reduced, which is 47% lower than that of pure PP. The PHRR of PP/OMMT is almost the same to that of PP/PP-*g*-MA/OMMT. As described above, the dispersion state of organoclay is different in PP/OMMT microcomposite and PP/PP-*g*-MA/OMMT nanocomposite. The similarity in PHRR for these two composites suggests that the dispersion state of the clay particles in the polymer matrix has a little influence on the flammability. In that way, the barrier effect of the silicate layers plays a minor role in the reduction of HRR for PCN.

Fig. 3 shows the mass loss plots recorded during cone calorimeter experiment. At the beginning, the mass loss for PP/PP-*g*-MA/OMMT nanocomposite and PP/OMMT microcomposite is greater than that for pure PP. Then the mass loss is slowed down in both composites compared to pure PP. The mass loss curve of PP/PP-*g*-MA blend is similar to that of pure PP, which has a little delay. The mass loss rate (MLR) curves are very similar to the HRR curves (not shown in the paper), so the reduction of the MLR is evidently the primary factor responsible for the lower HRR of the composites.

In order to understand the role of thermal-oxidative degradation in combustion, TGA measurements on the

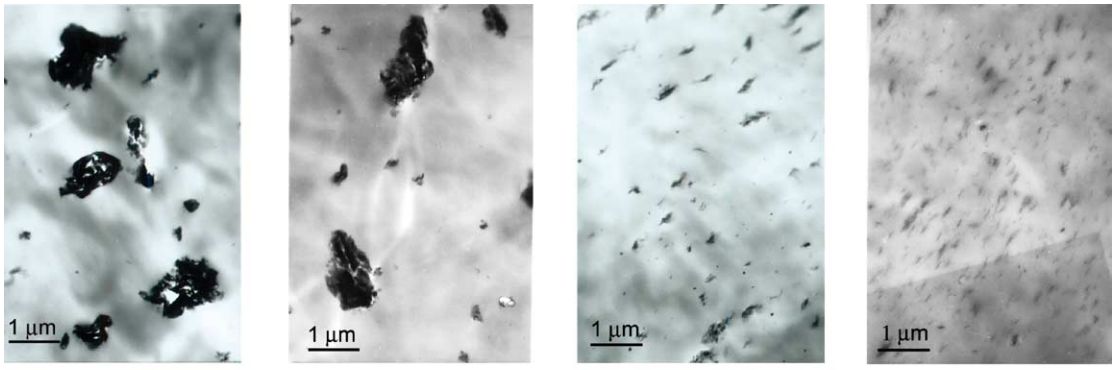

Fig. 1. TEM images of (A) PP/Na-MMT, (B) PP/H-MMT, (C) PP/OMMT, and (D) PP/PP-*g*-MA/OMMT.

Table 2
Cone calorimetric data of PP compounds at 35 kW/m^2

Sample	Ignition time (s)	Total heat evolved (MJ/m^2)	Peak HRR (kW/m^2)	Average EHC (MJ/kg)	Average SEA (m^2/kg)	Average CO yield (kg/kg)	Average CO_2 yield (kg/kg)	Residue yield (%)
Pure PP	52	219.4	1792	39.35	419.43	0.034	3.10	0
PP/C18	53	215.6	1463	38.90	456.50	0.034	3.08	2.86
PP/Na-MMT	45	216.7	1196	38.59	458.19	0.034	3.10	5.9
PP/H-MMT	42	211.4	1000	38.40	468.28	0.034	3.09	7.6
PP/OMMT	43	210.8	996	38.30	472.8	0.034	3.10	6.9
PP/PP-*g*-MA	55	219.8	1740	38.86	421.8	0.035	3.10	2.48
PP/PP-*g*-MA/OMMT	50	208.6	982	38.20	505.13	0.034	3.10	6.9

samples have been performed. Fig. 4 shows the TGA curves of pure PP, PP/PP-*g*-MA blend, PP/OMMT microcomposite and PP/PP-*g*-MA/OMMT nanocomposite in air atmosphere. Both PP/OMMT and PP/PP-*g*-MA/OMMT have a higher decomposition temperature in contrast to pure PP, while PP/PP-*g*-MA blend shows a little increase. TGA curve of PP/PP-*g*-MA/OMMT nanocomposite is very similar to that of PP/OMMT microcomposite. It suggests that the thermal-oxidative stability of PCN is unlikely to arise entirely from the barrier effect of the silicate layers themselves.

It is observed in Fig. 4 that the initial decomposition of both the composites is earlier than that of pure PP. The initial decomposition of the composites is more evident in isothermal oxidation experiments as shown in Fig. 5. At 200 °C in air atmosphere, the weight loss begins at about 3 min in both PP/OMMT microcomposite and PP/PP-*g*-MA/OMMT nanocomposite, while at 5 min in PP/PP-*g*-MA blend and 7 min in pure PP. It suggests that the addition of clay can catalyze the initial decomposition of PP matrix, which leads to the shortening of ignition time [9,10]. At the same time, the volatilization rate is slowed down in both composites compared to pure PP. The weight loss of the samples is well corresponding to their mass loss in cone calorimeter experiment, indicating that the thermal-oxidative degradation play an important role in the combustion of PP/clay nanocomposite.

3.2.2. The influence of MMT and alkylammonium

In order to understand the influence of organoclay in the nanocomposite, we investigated the effect of pristine clay and alkylammonium on flammability separately. Fig. 6 shows the HRR plots for pure PP, PP/C18 blend and PP/Na-MMT, PP/H-MMT, PP/OMMT microcomposite. The PHRR of PP/Na-MMT microcomposite is 33% lower than that of pure PP, while that of PP/H-MMT microcomposite is 44% lower. Although the dispersion state of clay particles in PP/H-MMT is the same to that in PP/Na-MMT, the PHRR of PP/H-MMT is much lower. The results indicate that the addition of clay can decrease the PHRR of PP matrix and that the acidic sites created on clay layers can make the PHRR lower.

It is well known that the thermal decomposition of alkylammonium salts in clay galleries could take place with the Hoffman mechanism leading to volatilization of ammonia and the corresponding olefin [21]:

$$LS^{-+}[NH_3–CH_2–(CH_2)_n–CH_3] \xrightarrow{\Delta} LS^{-}H^{+} + NH_3 + CH_2 = CH–(CH_2)_{n-1}–CH_3$$

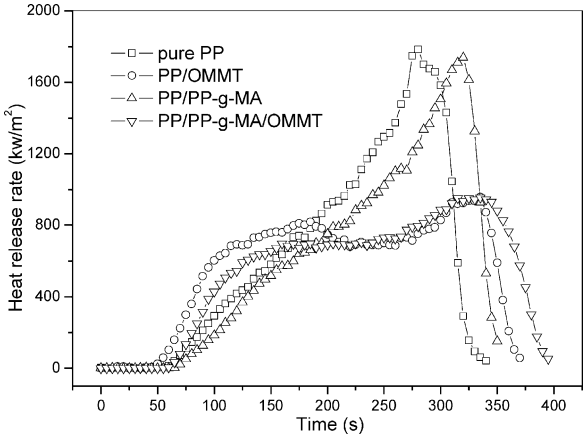

Fig. 2. HRR plots for pure PP, PP/PP-*g*-MA, PP/OMMT and PP/PP-*g*-MA/OMMT.

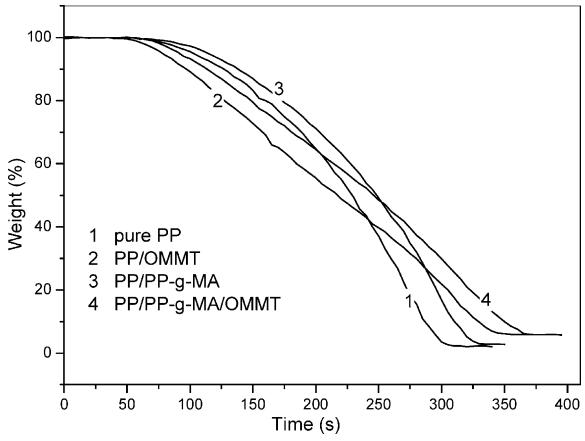

Fig. 3. Mass loss curves recorded during cone calorimeter experiment for pure PP, PP/PP-*g*-MA, PP/OMMT and PP/PP-*g*-MA/OMMT.

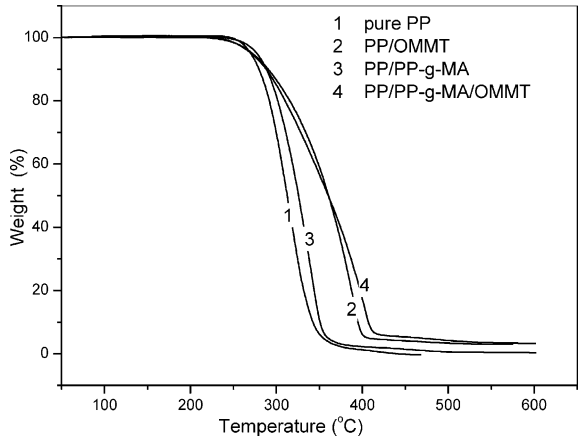

Fig. 4. TGA curves of pure PP, PP/PP-*g*-MA, PP/OMMT and PP/PP-*g*-MA/OMMT in air atmosphere.

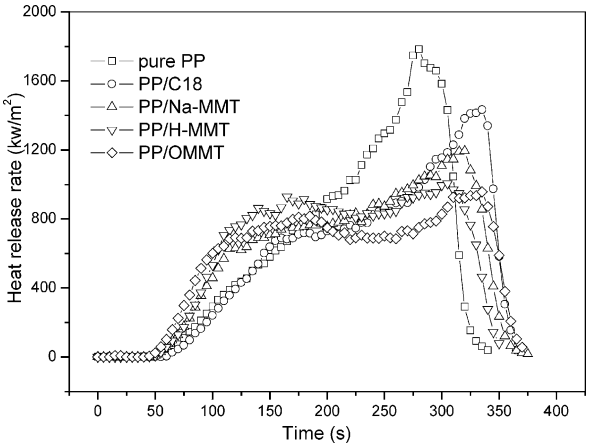

Fig. 6. HRR plots for pure PP, PP/C18, PP/Na-MMT, PP/H-MMT and PP/OMMT.

The acidic sites are thus created on the silicate layers during heating. The PHRR of PP/H-MMT is close to that of PP/OMMT and PP/PP-*g*-MA/OMMT though the clay dispersion state is different in these materials (compared Fig. 1(B)–(D)). It suggests that the acidic sites on clay layers play an important role in the reduction of HRR of PCN.

The addition of a tiny amount of alkylammonium salts (1.2 wt%) could also reduce the PHRR of polymer matrix. The PHRR of PP/C18 blend is 20% lower than that of pure PP. It is interesting that the HRR of PP/C18 blend is nearly the same to that of pure PP during the initial 100 s of the combustion. Moreover, the ignition time of PP/C18 blend is equal to that of pure PP. It proves effectively that the higher HRR of the nanocomposite during the initial combustion is not due to the volatiles from the decomposition of organic modification of clay, but due to clay itself.

The mass loss plots for pure PP, PP/C18 blend and PP/Na-MMT, PP/H-MMT, PP/OMMT microcomposite are shown in Fig. 7. At the beginning, the mass loss for all the composites is greater than that for pure PP. Afterwards, the mass loss is slowed down in all the composites. The initial mass loss of PP/C18 blend is nearly the same to that of pure PP and slowed down later.

The TGA curves of pure PP, PP/C18 blend and PP/Na-MMT, PP/H-MMT, PP/OMMT microcomposite in air atmosphere are shown in Fig. 8. The thermal decomposition temperature of PP/Na-MMT and PP/C18 are higher than that of pure PP. It is to say, the addition of pristine clay or alkylammonium salts can improve the thermal-oxidative stability of PP matrix. The TGA curve of PP/H-MMT is nearly concurrent to that of PP/OMMT, which is higher than that of PP/Na-MMT. It indicates that the acidic sites on clay layers can improve the thermal-oxidative stability higher. However, the initial decomposition of all the compounds is earlier than that of pure PP.

Fig. 9 shows isothermal TGA curves of pure PP, PP/C18 blend and PP/Na-MMT, PP/H-MMT, PP/OMMT microcomposite in air atmosphere at 200 °C. The initial decomposition of all the compounds is earlier than that of pure PP. The initial decomposition of PP/Na-MMT is more severe than that of PP/C18 and PP/OMMT. It indicates that the initial weight loss of the nanocomposite is not only due to the volatilization resulting from the decomposition of

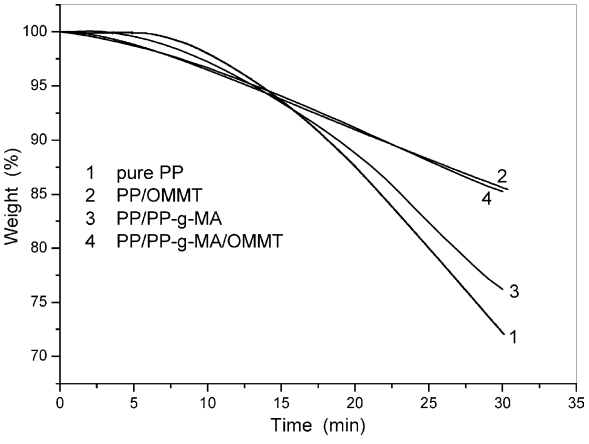

Fig. 5. Isothermal TGA curves of pure PP, PP/PP-*g*-MA, PP/OMMT and PP/PP-*g*-MA/OMMT (air atmosphere, 200 °C).

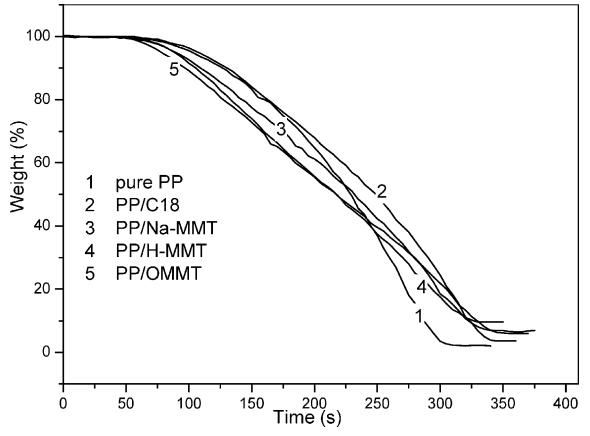

Fig. 7. Mass loss curves recorded during cone calorimeter experiment for pure PP, PP/C18, PP/Na-MMT, PP/H-MMT and PP/OMMT.

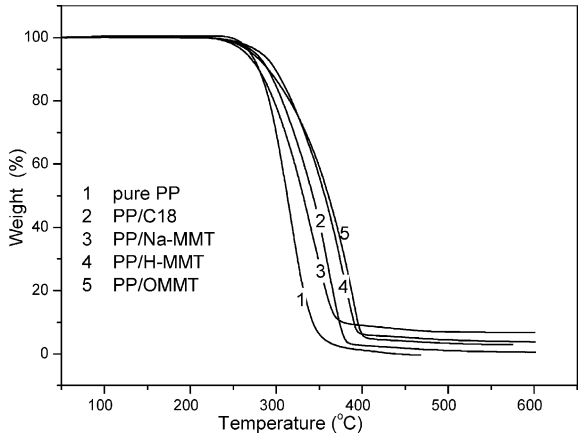

Fig. 8. TGA curves of pure PP, PP/C18, PP/Na-MMT, PP/H-MMT and PP/OMMT in air atmosphere.

organic modification, but also due to the oxidative decomposition of the PP matrix catalyzed by clay. Meanwhile, the volatilization rate is slowed down in all the compounds. Compared the curves of PP/H-MMT and PP/Na-MMT, the acidic sites on layered silicates can slow down the decomposition rate of PP matrix. The results in isothermal TGA experiment are consistent with the mass loss in cone calorimeter experiment (Fig. 7). It indicates that the reduction of HRR is mainly due to the delay of thermal-oxidative decomposition in PCN.

3.3. Characterization of char layer and char residue

The combustion behaviors of the tested samples are quite different. At the continuous heat flux of 35 kW/m^2, all the samples turned soft and generated volatile gases. Prior to ignition, pure PP melted and had a boiling surface, while all of the PP/clay composites did not melt and charred from the start. PP/C18 blend did not melt like pure PP and a lot of black flecks appeared on its soft surface. The performance of PP/PP-*g*-MA blend was similar to that of pure PP. Fig. 10 shows pictures of the samples prior to ignition and their

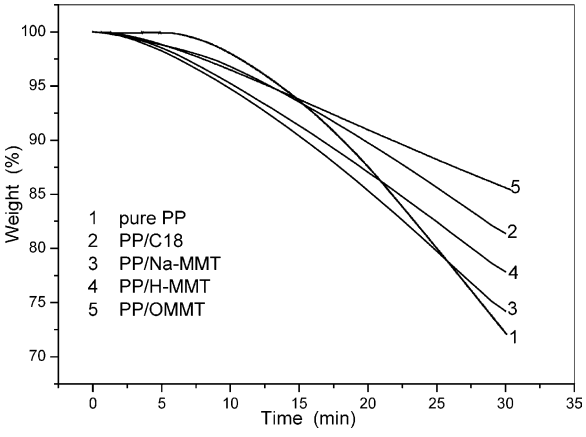

Fig. 9. Isothermal TGA curves of pure PP, PP/C18, PP/Na-MMT, PP/H-MMT and PP/OMMT (air atmosphere, 200 °C).

residues in the cone calorimetric experiment. As the mixture of volatile gases and oxygen exceeded the flammability limits under continuous spark, ignition occurred. During the combustion, some discontinuous dark floccules came into being on the surface of the PP/clay composites, and the blaze of the composites is gentler than that of pure PP. For PP/C18 blend, countless black flecks floated on the soft surface. At the end of combustion, pure PP burned out and nothing left on the sample pan, while PP/C18 and PP/PP-*g*-MA left only a little flecky char residue. PP/Na-MMT and PP/H-MMT left some gray ashes, and PP/OMMT and PP/PP-*g*-MA/OMMT left black block residues.

It was observed that a coat-like char formed on the surface of PP/PP-*g*-MA/OMMT nanocomposite at the stage prior to ignition and block char residue left after combustion. In order to clarify the structure and the composition of the char formed during combustion, the charred surface (prior to ignition) of the sample and the char residue were characterized by SEM, FT-IR and XRD.

The SEM micrographs of the char layer formed prior to ignition and char residue are shown in Fig. 11. At lower magnification (Fig. 11(A)), the char layer looks slick and continuous. It is like an overcoat covered on the nanocomposite. While at high magnification (Fig. 11(B)), the char layer appears harsh and poriferous. It looks like a lot of disordered flakes accumulated on the surface of the sample. However, the char residue shows a sponge-like structure (Fig. 11(C) and (D)) that is brittle and fragile.

Fig. 12 shows the FT-IR spectra of the nanocomposite and its char. The absorption at 1085 and 1035 cm^{-1} is Si–O stretching vibration of MMT. The absorption at 1455 and 1375 cm^{-1} is C–H bending vibration of polymer matrix, and the broad peak around 3000 cm^{-1} is C–H stretching vibration. In the char layer formed prior to ignition, the peaks of Si–O stretching have a dramatic increase compared to the bands of C–H bending and C–H stretching. Moreover, new peaks at 1719 and 1633 cm^{-1} appear, corresponding to the absorption of C=O stretching and C=C stretching. It indicates that the carbonaceous silicate char formed in the surface of the sample once the nanocomposite is ignited. It can be seen that, the char residue has almost no hydrocarbon absorption and contains a great amount of layered silicates.

Fig. 13 shows the XRD patterns of PP/PP-*g*-MA/OMMT nanocomposite and its char. As described in the previous work [22], the characteristic peak ($2\theta = 2.36°$) disappears in the nanocomposite. In the char layer formed prior to ignition, a new broad peak is observed at $2\theta = 4.5$–$6.3°$, corresponding to the *d*-spacing of 1.96–1.40 nm. It suggests that exfoliated layered silicates stacked randomly following decomposition of the polymer matrix. The XRD pattern of char residue exhibits a broad shoulder at about 2θ of 7°, corresponding to the *d*-spacing of 1.26 nm, suggesting that the clay layers in the char residue are partially re-aggregated and partially destroyed during the combustion.

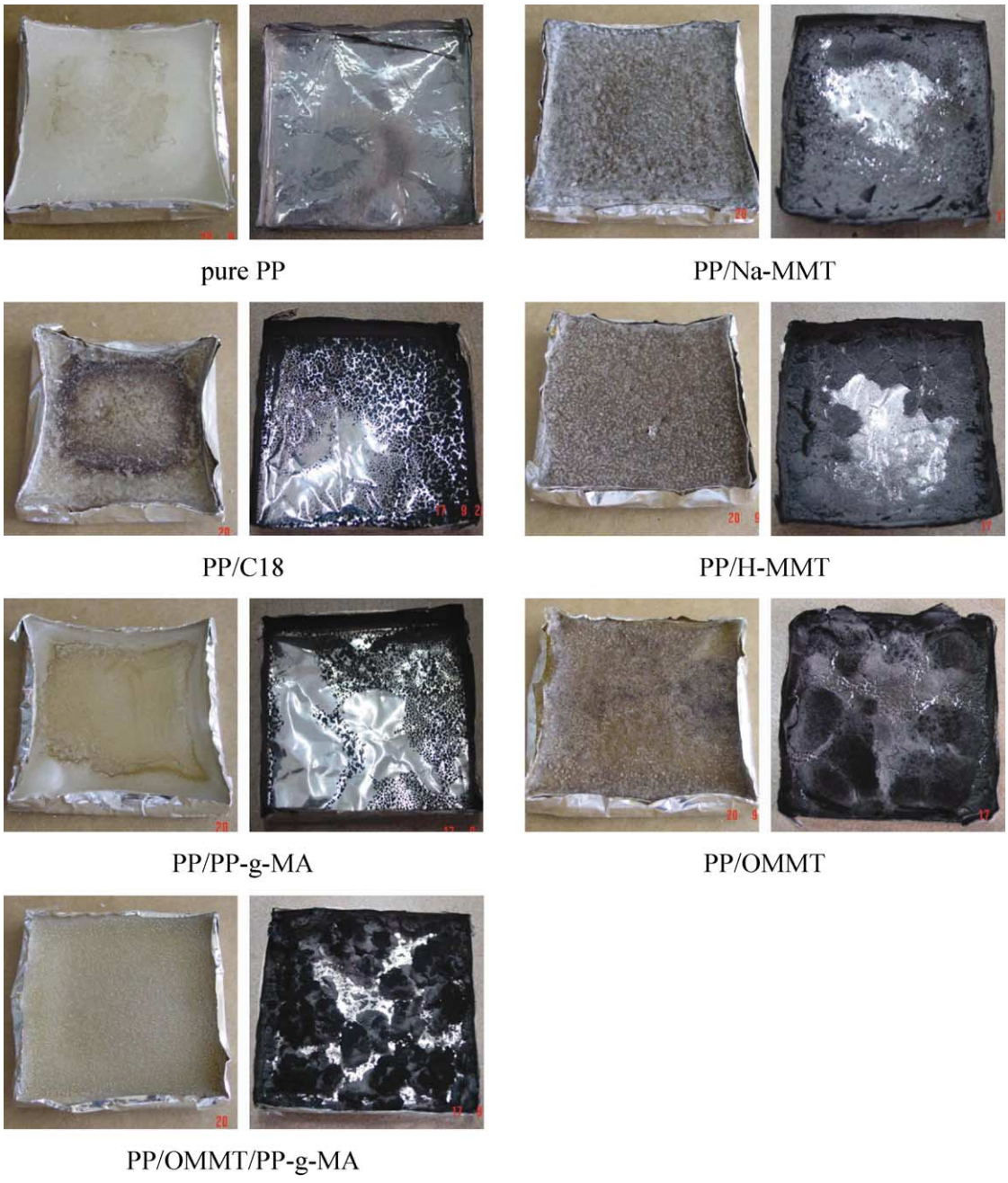

Fig. 10. Photographs of the samples prior to ignition (left) and their residues after combustion (right).

4. Discussion

As described above, the improvement in flammability properties of PP/clay nanocomposite is due to condensed-phase flame retardant mechanism. Compared to the results from the experiments of cone calorimetry and thermal-oxidative degradation, the decrease of HRR of the nanocomposite is mainly due to the delay of thermal-oxidative decomposition.

It was believed that, in the nanocomposites, the barrier effect of exfoliated layered silicates for volatiles played an important role in the delay of thermal-oxidative degradation and the decrease of HRR [3,4,6]. In the present work, the influence of compatibilizer (PP-*g*-MA), alkylammonium (C18), organoclay (OMMT), protonic clay (H-MMT) and pristine clay (Na-MMT) on the thermal-oxidative degradation and combustion of PP matrix is investigated respectively. Compared to pure PP, the mass loss rate of PP/clay composites has been slowed down. Moreover, the delay of mass loss in PP/H-MMT, PP/OMMT and the nanocomposite is quite similar, while the decrease of HRR in these samples is nearly the same. The dispersion state of layered silicates in these samples is very different, such as micro dispersion, immiscible/intercalated dispersion and

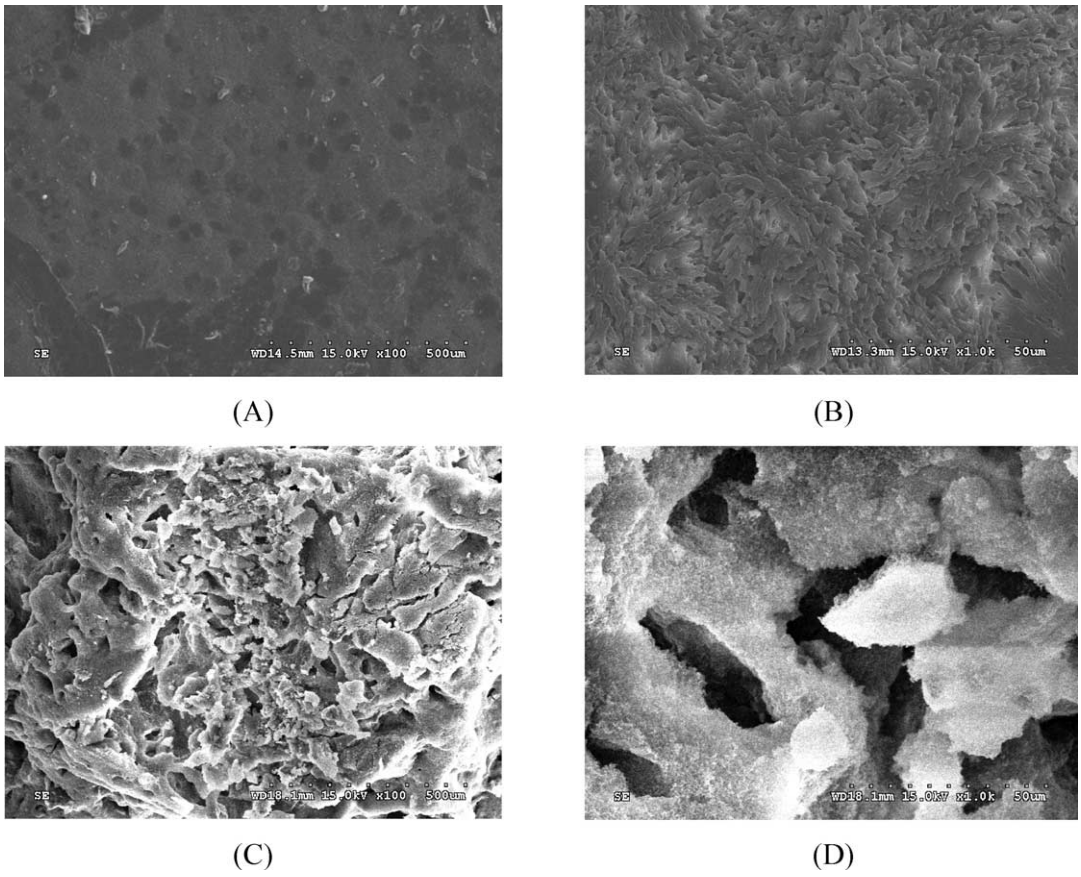

Fig. 11. SEM micrographs of PP/PP-*g*-MA/OMMT nanocomposite: The char layer formed prior to ignition at low magnification (A) and at high magnification (B); char residue after combustion at low magnification (C) and at high magnification (D).

nano dispersion. It indicates that the dispersion state of clay particles has a minor effect on thermal-oxidative stability and flammability of polymer matrix. In other words, the barrier effect of exfoliated layered silicates for volatiles offers a little contribution on the delay of thermal-oxidative degradation and the decrease of HRR in the nanocomposite.

Compared to pure PP, the ignition time is shorter and the initial HRR is higher in PP/clay composites. In the general view, the initial higher HRR and shorter ignition time in the nanocomposites is attributed to the release of the thermal degradation products of the organic treatment of the clay [3, 6]. However, the initial mass loss of PP/Na-MMT is more serious than that of PP/C18, while the initial HRR of PP/Na-MMT is higher than that of PP/C18. It is to say, in the

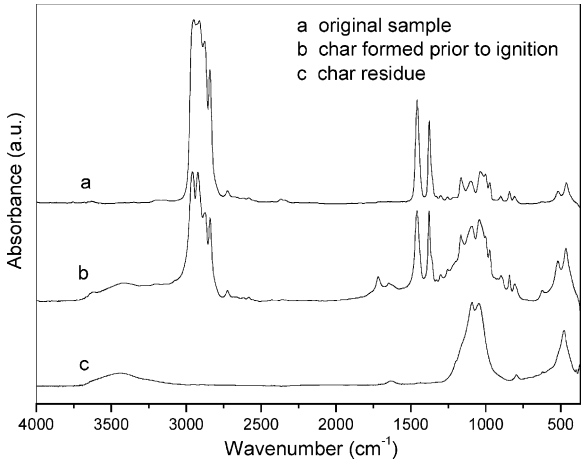

Fig. 12. FT-IR spectra of PP/PP-*g*-MA/OMMT nanocomposite (a) and its char formed prior to ignition (b) and char residue after combustion (c).

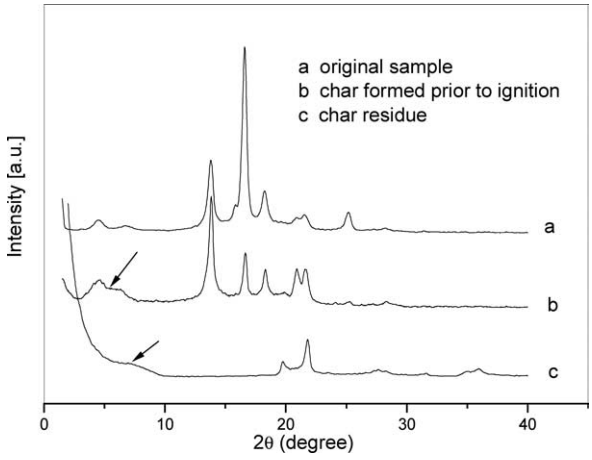

Fig. 13. XRD patterns of PP/PP-*g*-MA/OMMT nanocomposite (a) and its char layer formed prior to ignition (b) and char residue after combustion (c).

combustion test, the shorter ignition time and higher initial HRR of the nanocomposite is not only due to the volatiles from the decomposition of the organic modification of the clay, but due to the decomposition of the polymer matrix catalyzed by clay itself.

Pure PP did not char and had a boiling surface during the burning, while the nanocomposite charred from start. In a similar manner, PP/Na-MMT, PP/H-MMT and PP/OMMT microcomposites all charred from start. It suggests that the addition of pristine clay, protonic clay and organoclay can catalyze the formation of char layer on the surface of samples. As seen in the FT-IR spectra of the nanocomposite (Fig. 12), the broad absorption of C=O and C=C stretching present in this char layer (prior to ignition), which indicates oxidation, dehydrogenation and charring of polymer matrix. At the same time, the absorption of Si–O stretching of MMT has dramatically increased. The characterization of charred surface (prior to ignition) and char residue indicates that, the char formed during burning is a carbonaceous silicate char. This inorganic-rich ceramic-like char has better barrier properties for heat and volatiles [3,6,8]. The formation of char layer on the surface of samples is probably responsible for the delay of thermal-oxidative degradation and decrease of HRR in the nanocomposite.

At the same time, PP/clay composites did not melt during burning, while pure PP melted and had a boiling surface. It indicates that the viscosity of PP/clay composites is far higher than pure PP during the combustion. Kashiwagi et al. [8] have reported that polyamide 6/clay naonocomposite showed a significantly higher viscosity than polyamide 6 at high temperature. This suggests that there exists a physical crosslinking network structure composed of clay particles and polymer chains in these composites. This physical crosslinking effect can delay the thermal decomposition of polymer matrix. Interestingly, PP/C18 blend did not melt like pure PP during combustion, too. The thermal degradation of alkylammonium salts can lead to the generation of acid. It suggests that the acidic sites can catalyze the dehydrogenation and crosslinking of polymer chains. Therefore, the mass loss rate is lowed and HRR is decreased in PP/C18 blend. It is also the reason for that the mass loss rate and PHRR of PP/H-MMT is lower than that of PP/Na-MMT. These physical and chemical crosslinking can increase the thermal-oxidative stability and delay the thermal decomposition in the nanocomposite.

It has been reported that the complex crystallographic structure and habit of clay minerals result in some catalytic active sites, such as Bronsted acidic sites like the weakly acidic SiOH and strongly acidic bridging hydroxyl groups at the edge of the silicate layers, un-exchangeable transition metal ions in the galleries, and crystallographic defect sites within the layers [25]. The thermal degradation of organoclay can leads to acidic sites created on clay layers. At external heat flux, all these catalytic active sites can accept single electrons from donor molecules and form free radicals. On one hand, these active sites catalyze the initial decomposition of polymer matrix. It is why the ignition time is shorter and the initial HRR is higher for PP/clay nanocomposite. On the other hand, the active sites can catalyze the formation of a protective coat-like char on the nanocomposite. Moreover, the active sites can catalyze the dehydrogenation and crosslinking of polymer chains. Accordingly, the thermal-oxidative stability is increased and PHRR is decreased. The complete process is schematically shown in Fig. 14.

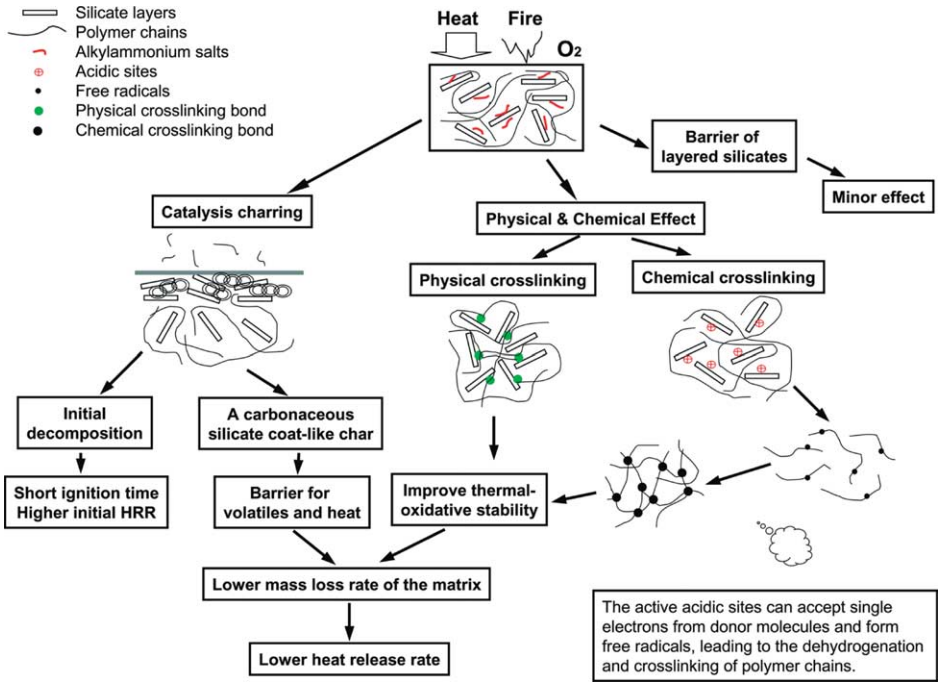

Fig. 14. Schematic representation of catalysis charring mechanism of PP/clay nanocomposite during combustion.

5. Conclusions

In this work, the combustion behavior and thermal-oxidative degradation of PP/clay nanocomposite and microcomposites have been investigated. The improvement in flammability properties of PP/clay nanocomposite is due to condensed-phase flame retardant mechanism. The decrease of HRR of the nanocomposite is mainly due to the delay of thermal-oxidative decomposition. Moreover, the shorter ignition time and higher initial HRR of the nanocomposite is not due to the volatilization from the decomposition of organic modifier in the organoclay, but due to the decomposition of the polymer matrix catalyzed by clay itself. The barrier effect of exfoliated layered silicates for volatiles offers a minor contribution on the delay of thermal-oxidative degradation and the decrease of HRR in the nanocomposite. The active sites on layered silicates and acidic sites created by the decomposition of organoclay can catalyze the dehydrogenation, crosslinking and charring of the nanocomposite. The protective coat-like char and physical–chemical crosslinking effect should be responsible for the delay of thermal-oxidative degradation and decrease of HRR in the nanocomposite.

Acknowledgements

This work was financially supported by the National Natural Science Foundation of China (Grant No. 50473054) and the Major Basic Research Projects of China (Grant No. 2003CB615600).

References

[1] Gilman JW, Kashiwagi T, Lichtenhan J. SAMPE J 1997;33:40.
[2] Gilman JW. Appl Clay Sci 1999;15:31.
[3] Gilman JW, Jackson CL, Morgan AB, Harris R, Manias E, Gannelis EP, et al. Chem Mater 2000;12:1866.
[4] Zhu J, Morgan AB, Lamelas FJ, Wilkie CA. Chem Mater 2001;13:3774.
[5] Zhu J, Uhl FM, Morgan AB, Wilkie CA. Chem Mater 2001;13:4649.
[6] Zanetti M, Kashiwagi T, Falqui L, Camino G. Chem Mater 2002;14:881.
[7] Zanetti M, Costa L. Polymer 2004;45:4367.
[8] Kashiwagi T, Harris RH, Zhang X, Briber RM, Cipriano BH, Raghavan SR, et al. Polymer 2004;45:881.
[9] Qin HL, Su QS, Zhang SM, Zhao B, Yang MS. Polymer 2003;44:7533.
[10] Qin HL, Zhang SM, Zhao CG, Feng M, Yang MS, Shu ZJ, et al. Polym Degrad Stab 2004;85:807.
[11] Zhao CG, Qin HL, Gong FL, Feng M, Zhang SM, Yang MS. Polym Degrad Stab 2005;87:183.
[12] Wang SF, Hu Y, Zong RW, Tang Y, Chen ZY, Fan WC. Appl Clay Sci 2004;25:49.
[13] Tang Y, Hu Y, Wang SF, Gui Z, Chen ZY, Fan WC. Polym Int 2003;52:1396.
[14] Okada A, Kawasumi M, Kurauchi T, Kamigaito O. Polym Prepr 1987;28:447.
[15] Giannelis EP. Adv Mater 1996;8:29.
[16] Garces JM, Moll DJ, Bicerano J, Fibiger R, Mcleod DG. Adv Mater 2000;12:1835.
[17] Ray SS, Okamoto M. Prog Polym Sci 2003;28:1539.
[18] Kojima Y, Usuki A, Kawasumi M, Okada A, Fukushima Y, Kurauchi T, et al. J Mater Res 1993;8:1185.
[19] Liu LM, Qi ZN, Zhu XG. J Appl Polym Sci 1999;71:1133.
[20] Burnside SD, Giannelis EP. Chem Mater 1995;7:1597.
[21] Zanetti M, Camino G, Reichert P, Mulhaupt R. Macromol Rapid Commun 2001;22:166.
[22] Qin HL, Zhang SM, Liu HJ, Xie SB, Yang MS, Shen DY. Polymer 2005;46:3149.
[23] Troitsch J. International plastic flammability handbook. 2nd ed. Munich: Hanser; 1990.
[24] Allen NS, Billingham NC, Calvert PD, Henman TJ, Stivala SS, Kimura J, et al. Degradation and stabilization of polyolefins. London: Applied Science; 1983.
[25] Xie W, Gao ZM, Pan WP, Hunter D, Singh A, Vaia R. Chem Mater 2001;13:2980.